Trabecular bone structure and anisotropy studies via diffusion-based MR

E. E. Sigmund[1], H. Cho[1], Y-Q. Song[1], S. Byrnes[1,2], P. Chen[1,2], E. X. Guo[3], T. Brown[3]

[1]NMR Research, Schlumberger-Doll Research, Ridgefield, CT, United States, [2]Department of Physics, Harvard University, Cambridge, MA, United States, [3]Department of Biomedical Engineering, Columbia University, New York, NY, United States

Background

Trabecular bone structure is of vital interest in the diagnosis and treatment of such bone disorders as osteoporosis. While bone mineral density (BMD), measured via dual x-ray absorptiometry (DXA), is the largest contributor to fracture risk, it is well known that structural issues contribute significantly as well[1, 2]. Trabecular bone specimens consist of a combination of rods and plates, and their mechanical strength is crucially dependent on their topology and anisotropy. A common characterization of bone architecture is microscopic computed tomography (μCT)[3]. A variety of MR methods have also been reported *in vitro* and *in vivo*, from pure linewidth or T2' [4] to high resolution microimaging[5, 6] to inter-molecular multiple quantum effects [7, 8]. In this work, we demonstrate a novel approach in which concrete geometrical information (specifically, a projected surface-to-volume ratio, S/V) is derived from MR diffusion measurements without the need of a high resolution image. The first technique uses the decay from diffusion in the internal field (DDIF)[9], i.e. internal field gradients within the trabecular bone are used to encode diffusive decay. The second technique measures time-dependent diffusion coefficients (D(t)) with pulsed field gradients (PFG)[10].

Methods

Eighteen bovine trabecular bone specimens were excised, and their marrow was removed and replaced with tap water. The samples were characterized with mechanical testing, microscopic computed tomography (μCT), and diffusion-based MR. Yield stress and bulk modulus were measured from a stress-strain curve of uniaxial compression. μCT images were collected for each sample (diameter~7 mm, length 8 mm) with a 34-μm 3D isotropic resolution. Two scalar parameters were calculated from the μCT images: (1) a projected $(S/V)_z$ and (2) the mean intercept length (MIL) along the 3 Cartesian axes. ^{1}H MR experiments were performed at 85 MHz (2 T) in a Nalorac superconducting magnet with a Bruker Biospec spectrometer and 3-axis gradient set (G_{max} = 1 T/m). The static field was applied along the cylindrical axis (z). DDIF data were obtained from a series of stimulated echoes with diffusion times from 1 ms to 10 s. A DDIF spectrum was generated through Laplace inversion [11]. PFG D(t) data were acquired with a 5 pulse (13 interval) stimulated echo sequence with internal field compensation[12], with applied gradients along 2 directions: one along the longitudinal axis (z), and one transverse to it (y). Diffusion times ranged from 200 ms to 3 s. For each sample and gradient direction, the set of time-dependent diffusion data D(t) was analyzed to obtain the S/V projected along that direction. Finally, a numerical calculation of the internal magnetic field was performed using the μCT images. The applied field was oriented along the longitudinal axis (z) in these calculations.

Results

Figure 1 shows μCT and MR results from the bone samples as a function of yield stress(YS). The images show 3D renderings of trabecular surfaces from cubical portions (2 mm x 2 mm x 2 mm) of the μCT images of several samples, demonstrating a progression from a network of rods (bottom left) to entangled rods and plates (top left) to highly oriented plates (top right). Also, isosurfaces of the internal magnetic field at 13 ppm above the applied field are shown (red) along with the structural images. The quantitative results from the diffusion-based NMR experiments (DDIF and D(t)) are as follows. The fast decaying portion of the DDIF distribution (20 ms < T < 0.5 s) was integrated to represent fast decay modes in each sample. This integral shows a gradual rise for weak bones, reaching a maximum at YS=6 MPa, and then decreases as the bones become stronger. The $(S/V)_{PFG,z}$ data derived from D(t) show an identical dependence on YS indicating that DDIF also measures S/V. From D(t) along two directions, structural anisotropy can be determined accurately. The weakest sample shows a low and isotropic S/V. The intermediate sample shows a high S/V with moderate anisotropy. The strongest sample shows a high S/V and high anisotropy. Both DDIF and $(S/V)_{PFG,z}$ show the same non-monotonic behavior, with a maximum near YS=6.0 MPa, whereas $(S/V)_{PFG,y}$ saturates at a constant value above that stress level. (S/V) and MIL derived from the μCT images showed similar trends (not shown) to the MR results.

Discussion

The DDIF distribution is determined by the internal field gradients in the sample. In trabecular bone, they exist primarily near the trabecular surfaces, with the largest gradients occurring near surfaces perpendicular to the applied field. DDIF detects the volume of these regions and thus probes the projected S/V along the applied field (z). The trend in the DDIF data is thus similar to the abundance of isosurfaces from one sample to the next in the image renderings. Also, the agreement of $(S/V)_{PFG,z}$ and DDIF fast weight supports this picture. Since $(S/V)_{PFG,z}$ is closely related to predictive indices such as mean intercept length[6] and trabecular number[13], the applicability of both MR diffusion techniques is clear. Two regimes of strength are evident in Figure 1: a weak regime (YS < 6 MPa) with an approximately constant anisotropy, and a strong regime (YS > 6 MPa) with an increasing anisotropy with yield stress. These structural regimes may have analogs in the course of bone evolution, either through natural growth or osteoporotic weakening. The diffusion-based NMR tools shown here thus have potential clinical application.

References

[1] Goldstein SA et. al. Calcified Tissue International, 1993; **53**(S1): S127 32, S132-3; [2] Kleerekoper M et. al. Calcified Tissue International, 1985; **37**: 594-597. [3] Pothuaud L et. al. Journal of Bone and Mineral Research, 2002; **17**(10): 1883-1895.; [4] Chung H et. al. Proc. Natl. Acad. Sci. USA, 1993; **90**: 10250-10254. [5] Chung HW et. al. Journal of Bone and Mineral Research, 1995; **10**(10): 1452-1461. [6] Majumdar S et. al. Bone, 1998; **22**(5): 445-454. ; [7] Bouchard LS et. al. Journal of Magnetic Resonance, 2005; **176**: 27-36. ; [8]Capuani S et.al. Magnetic Resonance in Medicine, 2001; **46**(4): 683-689. ; [9] Song Y-Q et. al. Nature(London), 2000; **406** 178-181. ; [10] Mitra PP et.al., Physical Review Lett, 1992; **68**:3555. ; [11]Song Y-Q et.al., Journal of Magnetic Resonance, 2002; **154**(2): 261-268. [12] Karlicek JRF et.al. Journal of Magnetic Resonance 1980; **37**(1):75. [13]Parfitt AM. Bone, 1992; **13**: S41-S47.

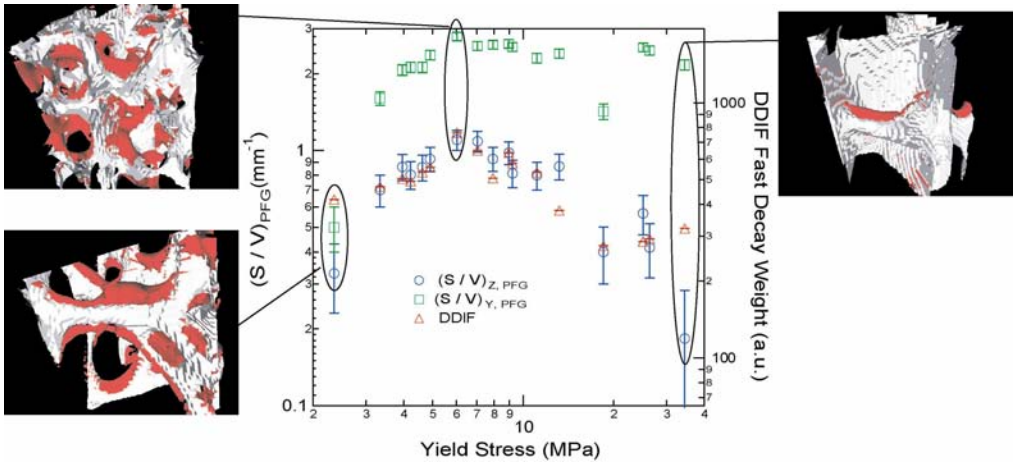

Figure 1 : Strength dependence of NMR (S/V) and DDIF measurements for bovine trabecular bone samples, along with rendered surfaces derived from μCT scans for 3 samples. The $(S/V)_z$ and DDIF data show similar trends, consistent with their common sensitivity to trabeculae perpendicular to the longitudinal (z) axis. The weaker bones (YS < 6 MPa) show constant anisotropy, while the stronger bones (YS > 6 MPa) show increasing anisotropy with strength. In the 3D renderings, trabecular bone surfaces are shown in white. Also shown in these images are isosurfaces from a calculation of the internal magnetic field in each structure (equal field value shown in each case of $\Delta B = B - B_0 = 6$ mG ~ 13 ppm).